Review Article

A narrative review of MRI acquisition for MR-guided-radiotherapy in prostate cancer

Jing Yuan[1]^, Darren M. C. Poon[2], Gladys Lo[3], Oi Lei Wong[1], Kin Yin Cheung[1], Siu Ki Yu[1]

[1]Medical Physics and Research Department, Hong Kong Sanatorium & Hospital, Hong Kong, China; [2]Comprehensive Oncology Centre, Hong Kong Sanatorium & Hospital, Hong Kong, China; [3]Department of Diagnostic & Interventional Radiology, Hong Kong Sanatorium & Hospital, Hong Kong, China

Contributions: (I) Conception and design: J Yuan, DMC Poon, G Lo; (II) Administrative support: OL Wong, KY Cheung, SK Yu; (III) Provision of study materials or patients: J Yuan, DMC Poon, G Lo; (IV) Collection and assembly of data: J Yuan, OL Wong; (V) Data analysis and interpretation: J Yuan, DMC Poon, G Lo; (VI) Manuscript writing: All authors; (VII) Final approval of manuscript: All authors.

Correspondence to: Jing Yuan, PhD. Medical Physics and Research Department, Hong Kong Sanatorium & Hospital, Happy Valley, Hong Kong, China. Email: jyuanbwh@gmail.com.

Abstract: Magnetic resonance guided radiotherapy (MRgRT), enabled by the clinical introduction of the integrated MRI and linear accelerator (MR-LINAC), is a novel technique for prostate cancer (PCa) treatment, promising to further improve clinical outcome and reduce toxicity. The role of prostate MRI has been greatly expanded from the traditional PCa diagnosis to also PCa screening, treatment and surveillance. Diagnostic prostate MRI has been relatively familiar in the community, particularly with the development of Prostate Imaging - Reporting and Data System (PI-RADS). But, on the other hand, the use of MRI in the emerging clinical practice of PCa MRgRT, which is substantially different from that in PCa diagnosis, has been so far sparsely presented in the medical literature. This review attempts to give a comprehensive overview of MRI acquisition techniques currently used in the clinical workflows of PCa MRgRT, from treatment planning to online treatment guidance, in order to promote MRI practice and research for PCa MRgRT. In particular, the major differences in the MRI acquisition of PCa MRgRT from that of diagnostic prostate MRI are demonstrated and explained. Limitations in the current MRI acquisition for PCa MRgRT are analyzed. The future developments of MRI in the PCa MRgRT are also discussed.

Keywords: Magnetic resonance-guided-radiotherapy (MRgRT); prostate cancer (PCa); integrated magnetic resonance imaging and linear accelerator (MR-LINAC); multi-parametric magnetic resonance imaging (mpMRI); diffusion weighted imaging (DWI)

Submitted Jul 07, 2021. Accepted for publication Aug 20, 2021.
doi: 10.21037/qims-21-697
View this article at: https://dx.doi.org/10.21037/qims-21-697

Introduction

Prostate cancer (PCa) is the second most common type of cancer among males only after lung cancer, and accounts for ~3.8% of all deaths caused in men in 2018 (1). Radiotherapy (RT) has been well proven and widely used as an effective and standard form of PCa treatment (2). To date, hypofractionation represents the RT standard for low- and intermediate-risk localized PCa in some clinical guidelines (3,4).

Magnetic resonance guided radiotherapy (MRgRT) (5-7), enabled by the recent clinical introduction of the integrated

^ ORCID: 0000-0001-8112-3608.

MRI and linear accelerator (MR-LINAC) systems (8-10), is a promising novel technique for PCa-RT, potentially offering advantages over the existing image-guided radiotherapy (IGRT) modalities. For example, MRgRT provides non-ionized superior soft-tissue image contrast to visualize the on-the-day targets and surrounding anatomies for treatment adaptation. MRI can be simultaneously acquired during radiation delivery for treatment gating and tracking. Moreover, functional or molecular imaging capability of MRI, has great potentials for radiotherapy treatment planning and response assessment (11).

The use of MRI in PCa diagnosis, including but not limited to tumor detection, localization, characterization, cancer staging, risk stratification and post-treatment evaluation, although is still evolving, has been relatively familiar to many clinicians and researchers (12). The development of Prostate Imaging - Reporting and Data System (PI-RADS) has greatly promoted global standardization and diminish variation in the acquisition, interpretation, and reporting of diagnostic prostate multiparametric MRI (mpMRI) examinations (13,14). In contrast, the emerging role of MRI in PCa-RT, is still much less introduced than diagnostic prostate MRI. Relevant publications are still sparse in the literature (15).

This review attempts to provide a comprehensive introduction and overview of MRI acquisition techniques currently used in the clinical workflows of PCa MRgRT, from treatment planning to online treatment guidance. This review orients more to the MRI part than to the RT part in the MRgRT. The major readers are assumed to be who have background knowledge on basic MRI principle and diagnostic prostate MRI, but might not be familiar with MRgRT. This review mainly focuses on MRI acquisition, but not on MRI reconstruction, image processing or interpretation. Special efforts are made to demonstrate and explain the major differences in the MRI acquisition for PCa MRgRT from the relatively well-known diagnostic prostate MRI. Limitations and pitfalls in the current MRI acquisition techniques for PCa MRgRT are presented. The future developments of MRI acquisition techniques in the PCa MRgRT are also discussed.

Literature search and information collection

Using the Medline/PubMed and Web of Science (WOS) databases, we performed a search with the keywords: magnetic resonance imaging or MRI and prostate cancer, and their combination with the following terms: diagnosis, radiotherapy, MR-LINAC, MR-guided radiotherapy, simulation, treatment planning, image guidance, and motion. Only full journal articles published in English were included. The literature search yielded a huge number of publication records. The literature selection for this review did not claim to be exhaustive but illustrative of the MRI acquisition techniques used in prostate cancer MRgRT. The authors had to subjectively select the most representative and most relevant studies in consensus, preferably published in the last 5 years, for review. The full articles were read and the relevant information on MRI acquisition were extracted.

Besides literature search, the user manual of "Marlin 1.5 T for Elekta Unity – Instructions for Use Release 5 Marlin" and unpublished documents such as the clinical protocols and research reports in our hospital were also used as information sources.

We present the following article in accordance with the Narrative Review Checklist (available at https://dx.doi.org/10.21037/qims-21-697).

MRI scanners in the MRgRT

Besides the normal diagnostic MRI scanner, MRgRT also involves the use of two different types of MRI scanners (*Figure 1*). They are the dedicated MRI-simulator (MR-sim) mainly for the offline use in the MRgRT treatment planning (16-19), and the MR-LINAC mainly for the online use in the MRgRT treatment fractions (8-10).

MR-sim and MR-LINAC have distinctive characteristics from the normal diagnostic MRI scanners (*Table 1*). Most MR-sims could be considered as the modified wide-bore (usually 70 cm) MRI scanners equipped with dedicated MRI-compatible RT accessories, rather than the completely new design of MRI. As such, MR-sims and diagnostic MRI scanners have the similar hardware configuration and performance of magnet, gradients, and built-in body radiofrequency (RF) coil. Their MRI console is also almost identical. Various MRI-compatible RT accessories are equipped with an MR-sim, such as the external 3D laser, flat patient couch top with standardized index, locating bars, RF coil holder or frame, and patient positioning devices (PPDs), mainly to implement MRI scan with the patient position as consistent as that in the RT treatment. Although all RF coils equipped with a diagnostic MRI scanner are also supported on an MR-sim, many of them are not used for MRI simulation scan due to their incompatibility with essential RT accessories. For example, diagnostic volumetric head coil is not compatible with thermoplastic

Figure 1 The three types of MRI scanners. Left: a normal 1.5 T diagnostic MRI scanner. Middle: a 1.5 T MRI-simulator. An anterior coil and its coil frame, as well as knee rest and ankle stock are shown. An external 3-dimensional laser is equipped. Right: a 1.5 T high field integrated MR-LINAC. There is neither in-bore nor external laser equipped with the MR-LINAC. MR-LINAC, MRI and linear accelerator system.

Table 1 The comparison of three types of MRI scanners

Configuration	Diagnostic MRI scanner	Dedicated MRI simulator	MR-LINAC
Field strength	1.5 T or 3T	1.5 T or 3T	0.35 T or 1.5 T
Bore diameter	60–70 cm	70 cm	70 cm
Patient couch	Curved surface (for patient comfort)	Flat couch top with index	Flat couch top with index
Positioning laser	In-bore 2D laser	External 3D laser	No laser (1.5 T)
Gradients	Powerful gradient amplitude and switching rate	Powerful gradient amplitude and switching rate	Compromised gradient amplitude and switching rate but better linearity (to minimize image distortion)
Build-in RF coil	Quadrature transmit-receive coil	Quadrature transmit-receive coil	Quadrature transmit-receive coil
RF coils	Various RF coils for imaging different anatomies	Limited coil options for simulation scan; usually use flexible surface coils, body array coil (anterior), spine array coil (posterior)	Only equipped with posterior coil and anterior coil on 1.5 T MR-LINAC; Coil size is smaller than their counterparts
Accessories	Optional	Coil holder (frame), locating bars, PPDs	Coil holder (frame), locating bars, PPDs
Console	MRI scan	MRI scan	MRI scan plus LINAC control
Sequence library	Supports many sequences with comprehensive scan protocols for different diagnostic scans in various anatomies	Contains diagnostic sequence library but seldom used for MRI simulation scan; customized MRI simulation scan protocols	Supports fewer sequences; standardized (fixed) scan protocol for online MRgRT scan

MR-LINAC, integrated MRI and linear accelerator system; RF, radiofrequency; PPD, patient positioning device; MRgRT, MR-guided radiotherapy.

immobilization mask (20,21).

Unlike MR-sims, MR-LINACs include distinctively designed MRI scanners to enable simultaneous MRI scan and radiation delivery on a single modality. To date, there are two commercial MR-LINAC systems, the low-field 0.35 T MR-LINAC (MRIdian Linac, ViewRay, Oakwood, CA, USA) (10) and the high field 1.5 T MR-LINAC (Elekta Unity, Elekta Instrument AB, Stockholm, Sweden) (9,22,23). In this article, we concentrate our illustration and discussion on the high field 1.5 T MR-LINAC, while the low field MR-LINAC is only briefly discussed. Magnet, gradients and built-in body coil on an MR-LINAC are so substantially modified, mainly for radiation beam passage, that their performances could be compromised or different from those

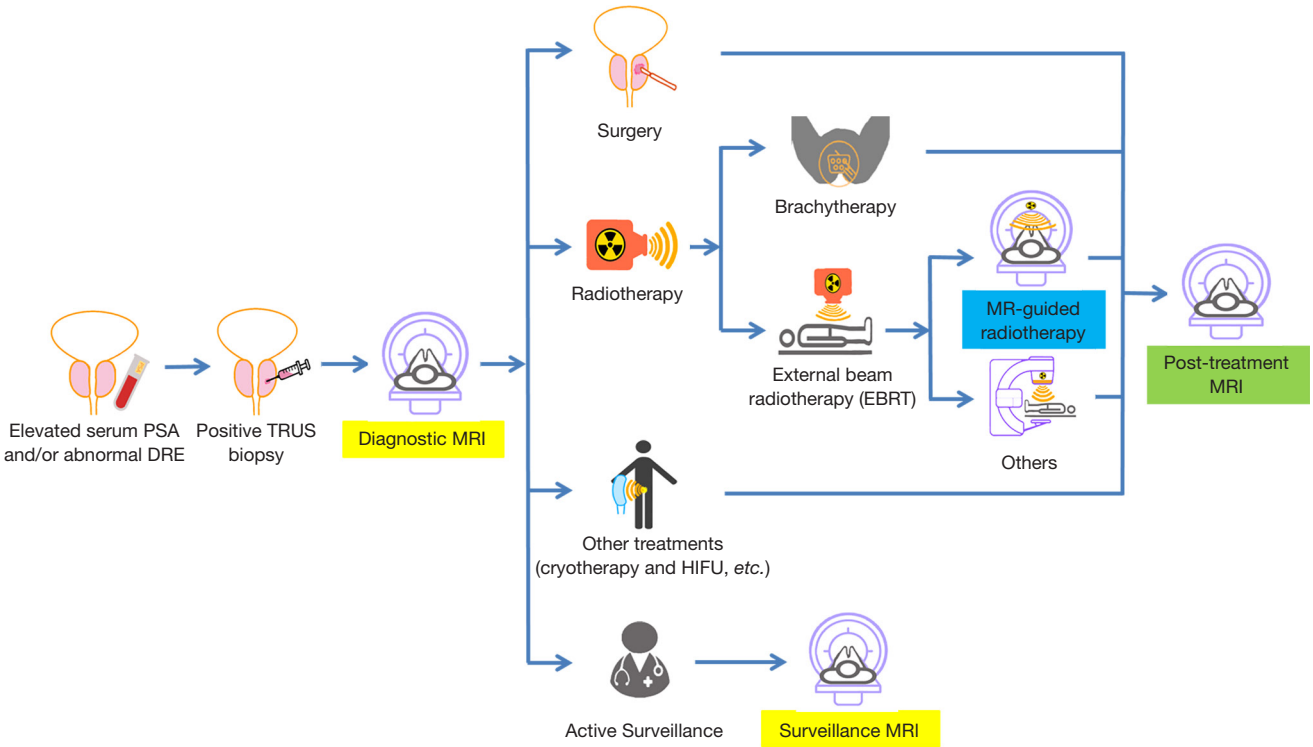

Figure 2 An illustration of the typical clinical course of a suspicious prostate cancer patient. The procedures involving the use of MRI in this entire course are represented by the blocks with colors. Yellow indicates the typical use of a diagnostic MRI scanner; Blue indicates that only integrated MR-LINAC can be used. Green indicates that all three types of MRI scanners could be used. PSA, prostate-specific antigen; DRE, digital rectal exam; TRUS, transrectal ultrasonography; HIFU, high intensity focused ultrasound; EBRT, external beam radiotherapy; MR-LINAC, MRI and linear accelerator system.

on a normal MRI scanner. For example, the gradient coils of a 1.5 T MR-LINAC are physically split to create a radiation window of 22 cm in the superior-inferior direction at the isocenter (24). This design substantially compromises the gradient performance to a maximum strength of 15 mT/m and a slew rate of 65 T/m/s in its clinical operation (25), against the typical maximum strength of >30 mT/m and slew rate of >125 T/m/s on a modern 1.5 T diagnostic MRI scanner. A 1.5 T MR-LINAC is only equipped with two 4-channel RF coils, i.e., anterior coil and posterior coil, for MRI scan. Due to its compromised hardware performance, fewer sequences are currently supported. For a 1.5 T MR-LINAC, it has two consoles. One is the stand-alone MRI console, which is highly similar to that on a normal MRI scanner, and can only be used for MRI scan but not for LINAC control. The other is the treatment console that has the full control on the LINAC but has limited interaction with MRI acquisition. On the treatment console, the pulse sequences in the built-in protocol libraries can be selected to trigger MRI acquisition. The acquired images are immediately transferred to the treatment console for subsequent clinical tasks such as image co-registration, anatomical contouring, and plan adaptation. Note that only the built-in sequences can be selected and image parameter adjustment is not allowed on the treatment console.

Typical clinical scenario and workflow of MRgRT in prostate cancer

There is no well recognized consensus on the optimal patient selection for prostate cancer MRgRT (26). Here we just take an example of the typical clinical course of a suspicious PCa patient who has a rising prostate-specific antigen (PSA) and/or an abnormal digital rectal exam (DRE) (*Figure 2*). Such a patient usually undergoes transrectal ultrasonography (TRUS) guided prostate biopsy. A positive TRUS biopsy result usually leads to the subsequent diagnostic MRI to detect, characterize and stage

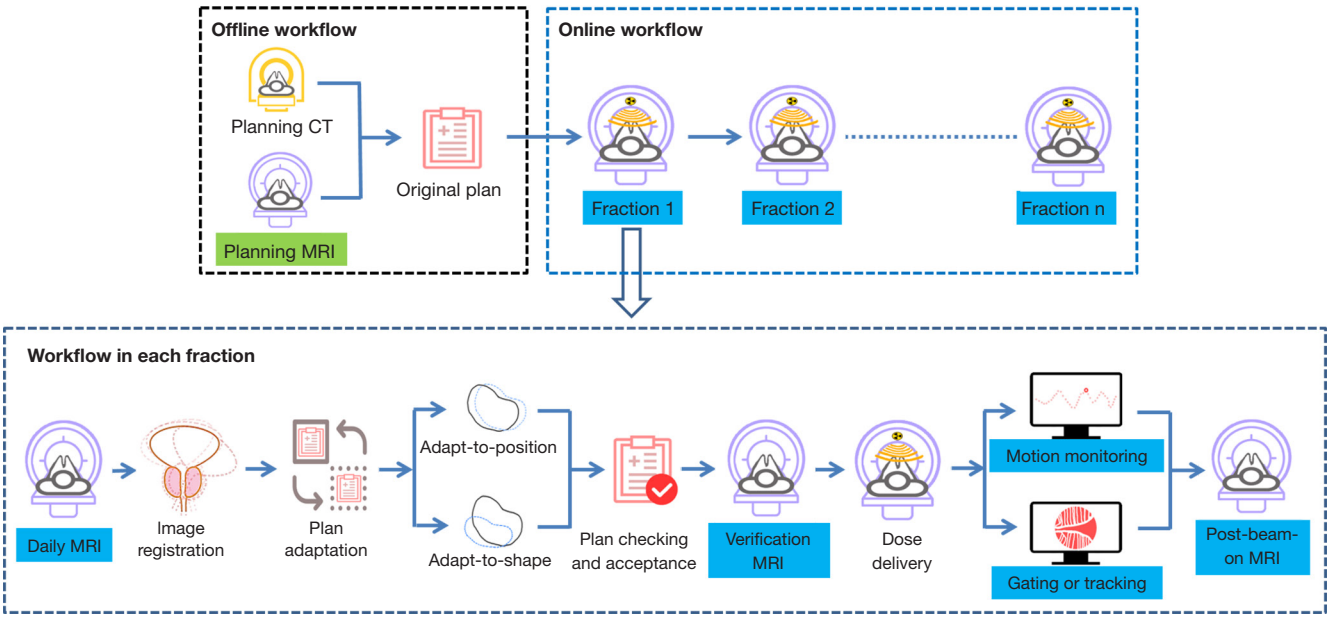

Figure 3 The typical clinical workflow of the MRgRT in the prostate cancer. The procedures involving the use of MRI are represented by the blocks with colors. Green indicates that all three types of MRI scanners could be used. Blue indicates that only integrated MR-LINAC can be used. MRgRT, MR-guided radiotherapy; MR-LINAC, MRI and linear accelerator system.

the possible PCa for further clinical decision on treatment or surveillance. The surveillance MRI should be useful for a PCa patient who undergoes active surveillance instead of any treatment (27). No matter what treatment is determined and conducted, post-treatment MRI might be used for treatment assessment (11). The procedures involving the use of MRI in this entire course are represented by the blocks with colors in *Figure 2*. Different colors indicate the MRI scanners applicable for that procedure.

If MRgRT is determined for a PCa patient, he will normally undergo the typical MRgRT clinical workflow as illustrated in *Figure 3*. This workflow is divided into the offline session of MRgRT treatment planning, and the online session of multiple MRgRT treatment fractions that can be only conducted on an MR-LINAC. Planning MRI is acquired mainly to assist anatomical delineation, target definition and treatment margin setting by fusing with planning CT (16,28). In the online MRgRT session, online MRI is acquired multiple times on an MR-LINAC with different purposes during each MRgRT fraction (23,29). A daily MRI is first acquired to obtain the on-the-day anatomical information, which is co-registered to the original treatment plan to determine whether plan adaptation is needed. If plan adaptation is decided, either adapt-to-position (via rigid registration to the original plan) or adapt-to-shape (via deformable registration to the original plan) is conducted (23). During this online plan adaptation, the patient remains in the MR-LINAC, instructed not to move. After finishing plan checking and acceptance, a verification MRI is then acquired to ensure that the patient does not move out of tolerance, and proceeds with dose delivery (30). During the dose delivery, or called beam-on time, MRI can be optionally acquired to monitor the possible patient position change (30), or to perform real-time dose gating or tracking (31). Gating or tracking by utilizing the real-time superior-contrast MR images is a great advantage of MRgRT over conventional IGRT for more precise dose delivery. This function is currently implemented only on the 0.35 T MR-LINAC but not yet on the 1.5 T MR-LINAC. Finally, after the dose delivery, post-beam-on MRI may be optionally acquired.

As shown in *Figure 2*, many PCa patients might have undergone diagnostic MRI prior to their MRgRT. An often asked question is whether the diagnostic prostate MRI could be directly used for MRgRT planning to omit an additional planning MRI scan. The answer might depend on the treatment precision to achieve in the MRgRT (32,33). A dedicated planning MRI acquired in the patient position as close as possible to that in the MRgRT could

Table 2 Major differences in the patient preparation and setup for three MRI modalities

Characteristic	Diagnostic MRI	MRgRT planning MRI	MRgRT online MRI
Clinical purposes	Detection	Target delineation	Position verification
	Characterization	OAR delineation	Treatment adaptation
	Staging	Margin setting	Guidance (motion monitoring, gating, tracking etc.)
MRI scanner	Normal MRI scanner	Normal MRI scanner	MR-LINAC
		Dedicated MR-sim (preferable)	
		MR-LINAC	
Scan timing	>6 weeks after TRUS biopsy	The interval between planning CT and planning MRI as short as possible	As short as possible after planning CT and planning MRI
Patient safety	MRI safety	MRI safety	MRI safety
			Radiation safety
Patient position	Supine, flexible	Supine, as consistent as possible with MRgRT treatment position	Supine, MRgRT treatment position
Patient alignment	2D alignment using in-bore laser	3D alignment using external laser	Laser-free physical position alignment
Bladder control	No need	Consistent bladder volume desirable	Consistent bladder volume desirable
Endorectal preparation	ERC inserted (preferable)	Endorectal balloon inserted (preferable)	Endorectal balloon inserted (preferable)
RF coil	Body array coil (essential), ERC (preferable)	Body array coil (essential, without body touching), ERC (no need)	Body array coil (essential, without body touching), ERC (no need and not supported)
Contrast agent	Usually needed (for DCE-MRI)	Usually no need	Usually not allowed

MRgRT, MR-guided radiotherapy; MR-LINAC, integrated MRI and linear accelerator system; MR-sim, MR-simulator; TRUS, transrectal ultrasonography; ERC, endorectal coil; DCE-MRI, dynamic-contrast enhanced MRI.

greatly reduce the registration error and uncertainty to the planning CT, so as to benefit dose calculation and MRgRT precision (18,34,35). Another related question is whether an MR-LINAC is preferable for planning MRI scan over an MRI-sim. The use of MR-LINAC for planning MRI has pros and cons. It has the advantages of the identical patient position on a single scanner, identical hardware-dependent image distortion profile, and similar MR image appearances to facilitate better image co-registration. But, the extremely high cost of MR-LINAC might reduce the cost-effectiveness of planning MRI (36). Meanwhile, considering the compromised hardware performance and limited sequences on the MR-LINAC, its imaging capability or image quality might be compromised. For example, image quality of diffusion-weighted imaging (DWI) on an MR-LINAC, such as signal-to-noise ratio (SNR) and artifacts, could be poorer than that on an MR-sims (25,37).

Patient preparation and MRI scan consideration

The planning MRI and online MRI in PCa MRgRT have substantially different patient preparation/setup and special consideration factors for MRI scan.

Table 2 summarizes some major differences in the patient preparation and setup for the three MRI modalities. Among these differences, bladder control is considered important for MRgRT MRI. Full bladder control is conventionally applied in PCa radiotherapy to better spare bladder and small bowel, but subjects to patient capability. Consistent bladder volume is also desirable to achieve more precise dose delivery during the treatment fractions (38,39). In terms of RF coil use, a body array coil is commonly used, but the coil should not touch the patient body to cause deformation, which might introduce extra registration errors in treatment planning (17). An endorectal coil (ERC) is often used for diagnostic prostate MRI in order to

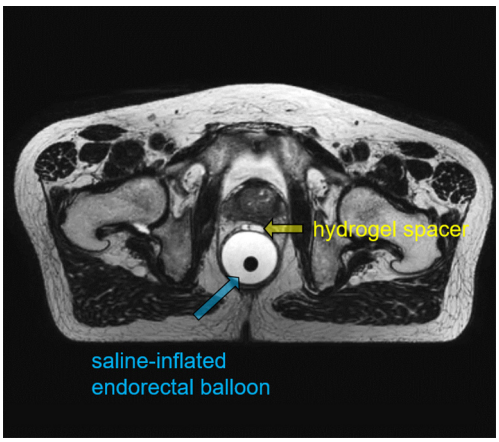

Figure 4 A T2-weighted planning MRI of a prostate cancer patient showing the insertion of the saline-inflated endorectal balloon in the rectum to immobilize the prostate, and the injected hydrogel spacer to increase the distance between the prostate and rectum.

improve the local SNR for better tumor localization (40). In contrast, an endorectal balloon is often used instead for MRgRT MRI, helping to limit prostatic motion during dose delivery so as to minimize rectal toxicity (41). Invasive fiducial markers, which are commonly implanted into the prostate in the conventional IGRT, are no longer needed in the PCa MRgRT (26). Hydrogel spacer could also be injected before PCa MRgRT to increase the distance between the prostate and rectum, thus to minimize the radiation dose delivered to rectum (42,43). *Figure 4* shows the T2W planning MRI of a PCa MRgRT patient, in which the saline-inflated endorectal balloon and the injected hydrogel spacer are well visualized. Regarding contrast agent use, gadolinium-based contrast agent (GBCA) is usually administered to conduct dynamic-contrast enhanced MRI (DCE-MRI) as well as post-contrast T1W MRI in the diagnostic scan (44), but might not be needed in the MRgRT planning MRI scan, especially when diagnostic MRI has been available. Furthermore, GBCA administration is usually not allowed for online MRI in the multiple MRgRT fractions.

Due to the distinctive clinical purposes of MRI in PCa MRgRT, MRI acquisition in the PCa MRgRT has special considerations on its scan protocol, making it substantially different from that in the diagnostic prostate MRI. *Table 3* summarizes some major scan protocol considerations for MRI in PCa MRgRT in comparison to diagnostic MRI (16,17). Note that many of these special considerations are also applicable for MRgRT in other regions for different diseases. For example, geometric fidelity is of utmost importance for all imaging, including but not limited to MRI, for radiotherapy purpose (45-47). Thus, image distortion correction should be always enabled for MRI scans in the MRgRT. Meanwhile, neither slice gap nor tilting is applied for RT imaging.

The use of isotropic 3D sequences in PCa MRgRT would greatly ease image reformatting and anatomy contouring in the orthogonal planes. It also saves the scan time to obtain coronal or sagittal prostate view by using the 2D sequences (48). Another benefit of 3D sequence is that its image distortion profile is slightly better than that of its 2D sequence counterpart (45). For these reasons, 3D sequences are highly preferable and more frequently used in the MRI scan for MRgRT than in the diagnostic MRI scan.

MRI in the PCa MRgRT also differs from diagnostic prostate MRI in its FOV. In the diagnostic prostate MRI, there should be minimally one sequence to have sufficiently large FOV that permits pelvic lymph node assessment to the level of the aortic bifurcation according to the PI-RADS. Other sequences usually have small FOVs (~20 cm) to focus on prostate and surrounding anatomies (48). In contrast, in the PCa MRgRT, most sequences, in particular of T2W, require a FOV larger than the body profile in the pelvis (usually >40 cm) and a wide superior-inferior coverage (at least wider than the maximum superior-inferior radiation width of the MR-LINAC, i.e., 22 cm for a 1.5 T MR-LINAC) to include not only prostate but also many organs-at-risk (OARs) to be delineated in the planning.

In terms of scan duration, MRgRT planning MRI scan could be reasonably short by fully utilizing the prior knowledge of lesion malignancy, location, size and extension, obtained in the diagnostic MRI for many PCa patients. MRgRT online MRI also desires short MRI scans to minimize the chance of patient position change and to enhance treatment efficiency for higher patient throughput. Real-time imaging capability are critically demanded in the MRgRT online MRI for motion monitoring and treatment gating/tracking, but they are not mandatory in either diagnostic or planning MRI mainly for retrospective viewing.

MRI scan protocol in PCa MRgRT

The typical scan protocol of the diagnostic prostate MRI is mainly multi-parametric MRI (mpMRI) or the simplified bi-parametric MRI (bpMRI), which has been well described

Table 3 The comparison of MRI scan protocol considerations

Scan protocol consideration	Diagnostic MRI	MRgRT planning MRI	MRgRT online MRI
Sequence type	2D sequence preferable (for T2W)	3D sequence preferable (for isotropic voxel)	3D sequence preferable (for isotropic voxel)
Image orientation	Usually transversal and coronal, tilting is allowed	Usually transversal only, tilting usually not allowed	Usually transversal only, tilting usually not allowed
FOV	Small FOV is allowed (to focus on prostate)	Large FOV is often required (for prostate and OARs coverage)	Large FOV is often required (for prostate and OARs coverage)
Image distortion	Could be tolerated (as long as diagnosis not compromised), distortion correction is optional	Must be minimized (e.g., by SE sequences and high receive bandwidth), always enable distortion correction (preferable in 3D)	Must be minimized (e.g., by SE sequences and high receive bandwidth), always enable distortion correction (preferable in 3D)
Image uniformity	Could be tolerated (as long as diagnosis not compromised)	High uniformity preferable (to facilitate anatomy segmentation)	High uniformity preferable (to facilitate anatomy segmentation)
Special image artifacts	No special	No special	Possible image artifacts due to gantry rotation and irradiation should be considered
Scan duration	Reasonably long (for comprehensive diagnosis)	Reasonably short	Short scan preferable (to minimize positional change and maximize treatment efficiency)
Imaging latency	Long latency is usually tolerated (for retrospective viewing and reading)	Long latency is usually tolerated (for retrospective viewing and reading)	Short latency is preferable, real-time capability is mandatory for motion monitoring, gating and tracking

MRgRT, MR-guided radiotherapy; T2W, T2-weighted; FOV, field-of-view; OAR, organ-at-risk; SE, spin echo; FOV, field-of-view.

elsewhere in PI-RADS and many other literatures (12,49-53).

Despite the increasing use of MRI in PCa radiotherapy treatment planning, its scan protocol has not yet been well established or standardized. In principle, if a recent diagnostic MRI is not available for a PCa patient for MRgRT, the full mpMRI protocol should be included in his planning MRI, with necessary modifications based on the abovementioned special scan considerations for MRI in MRgRT. On the contrary, the scan protocol of MRgRT planning MRI can be greatly simplified by fully utilizing the prior knowledge obtained in the recent diagnostic prostate MRI.

Unlike MR-sims, MRgRT online MRI are highly standardized on the 1.5 T MR-LINACs, since only the built-in sequences can be selected for either daily MRI, verification MRI or motion monitoring MRI. The only exemption is the MRI acquisition conducted in the stand-alone MRI console, e.g., post-beam-on MRI, which allows sequence and imaging parameter change, but cannot interact with the LINAC.

The typical MRI pulse sequences used in the three MRI modalities are listed in *Table 4*. The role of each MRI sequence in the PCa MRgRT is further described as follows.

T2W MRI

A T2W sequence is essential and utmost important in the PCa MRgRT planning MRI (54-56). T2W images are most useful to discern prostatic zonal anatomy and to assess intra-prostatic abnormalities. Moreover, T2W images are invaluable to assess seminal vesicle invasion and extra-prostatic extension (EPE), which are critically important for the definition of clinical target volume (CTV) in MRgRT treatment planning (56). T2W MRI also has added value on the delineation of other OARs such as rectum, penile bulb, seminal vesicle, and sacral plexus compared to planning CT (54,56). *Figure 5* shows the appearances of prostate and various OARs in the T2W MRgRT planning MRI.

It is also worth noting that detection and localization of intra-prostatic tumors in the MRgRT planning MRI might

Table 4 The typical MRI pulse sequences used in the three MRI modalities

Pulse sequences	Diagnostic MRI	MRgRT planning MRI	MRgRT online MRI
Typical protocols	mpMRI or bpMRI	Customized	Fixed T2W plus orthogonal CINE
T2W MRI (TSE)	2D-TSE preferable	3D-TSE preferable	3D-TSE fixed
	High resolution	High resolution	Low resolution
	Essential	Essential	Essential
T1W MRI (TSE or GRE)	2D or 3D	2D or 3D (preferable)	Available but seldom used
	High resolution	High resolution	Optional
	Preferable	Optional	
DWI	Essential	Optional for whole prostate irradiation	Not clinical available
		Preferable for DIL dose escalation	Potentially useful
DCE-MRI	Essential for mpMRI	Optional	Not used (GBCA usually not allowable)
		Unfavorable when diagnostic mpMRI available	
Proton MRS	Unfavorable (limited value)	Unfavorable (limited value)	Not clinical available
bSSFP	Not used	Essential for 0.35 T MRgRT	Essential for online motion MRI (both 0.35 T and 1.5 T)
		Optional for motion characterization (both 0.35 T and 1.5 T)	Essential for gating and tracking (only at 0.35 T)
Other sequences	CEST, BOLD, DTI, USPIO, IVIM, MRSI, polarized 13C-pyruvate MRI etc.	T2*W, Dixon (for synthetic CT generation) etc.	Not clinical available
	Optional	Optional	

MRgRT, MR-guided radiotherapy; T2W, T2-weighted; T1W, T1-weighted; mpMRI, multi-parametric MRI; bpMRI, bi-parametric MRI; CINE, not an abbreviation, a repeated acquisition MRI technique to capture dynamic motion; TSE, turbo spin echo; GRE, gradient recalled echo; DWI, diffusion-weighted imaging; DIL, dominant intra-prostatic lesion; GBCA, gadolinium-based contrast agent; CEST, chemical exchange saturation transfer; BOLD, blood-oxygen-level-dependent; DTI, diffusion tensor imaging; USPIO; ultrasmall superparamagnetic iron oxide; IVIM, intravoxel incoherent motion, MRSI, magnetic resonance spectroscopic imaging.

not be as important as that in the diagnostic prostate MRI. Because of the abovementioned special considerations on MRI scan in the PCa MRgRT, the scan protocol of the T2W MRgRT planning MRI might not be able to meet all technical requirements specified in the PI-RADS v2.1, so compromises lesion visualization. For example, PI-RADS requires the in-plane spatial resolution of ≤0.7 mm in phase encoding and ≤0.4 mm in frequency encoding for T2W MRI in a FOV of 12–20 cm. But it is technically challenging for a T2W MRgRT planning MRI to obtain such a high resolution with the large FOV of ≥40 cm and sufficient SNR in a reasonable scan duration (of several minutes) using an isotropic 3D-T2W-TSE sequence. Even with 3T diagnostic mpMRI, a recent study showed that a substantial proportion of PCa lesions, in particular of small, low-grade, multifocal and non-index tumors with lower PSA density, could be missed (at least one clinically significant focus in 34% patients (n=588) overall, and in 45% of patients with multifocal lesions) (57). Therefore, it is not surprising that individual PCa foci could not be all visualized in the single T2W MRgRT planning MRI, particularly at 1.5 T with MR-LINAC. But, because of the multi-focal and heterogeneous nature of PCa (58), the whole prostate irradiation is still the standard and mainstream in PCa radiotherapy practice including the PCa MRgRT. As such, even with the limitation of individual tumor visualization on T2W MRI, the single-parametric T2W scan protocol might be acceptable to fulfill the minimal requirements on prostate and OARs contouring in MRgRT treatment planning, in particular when the recent diagnostic MRI is available.

One major difference of the T2W MRI in MRgRT

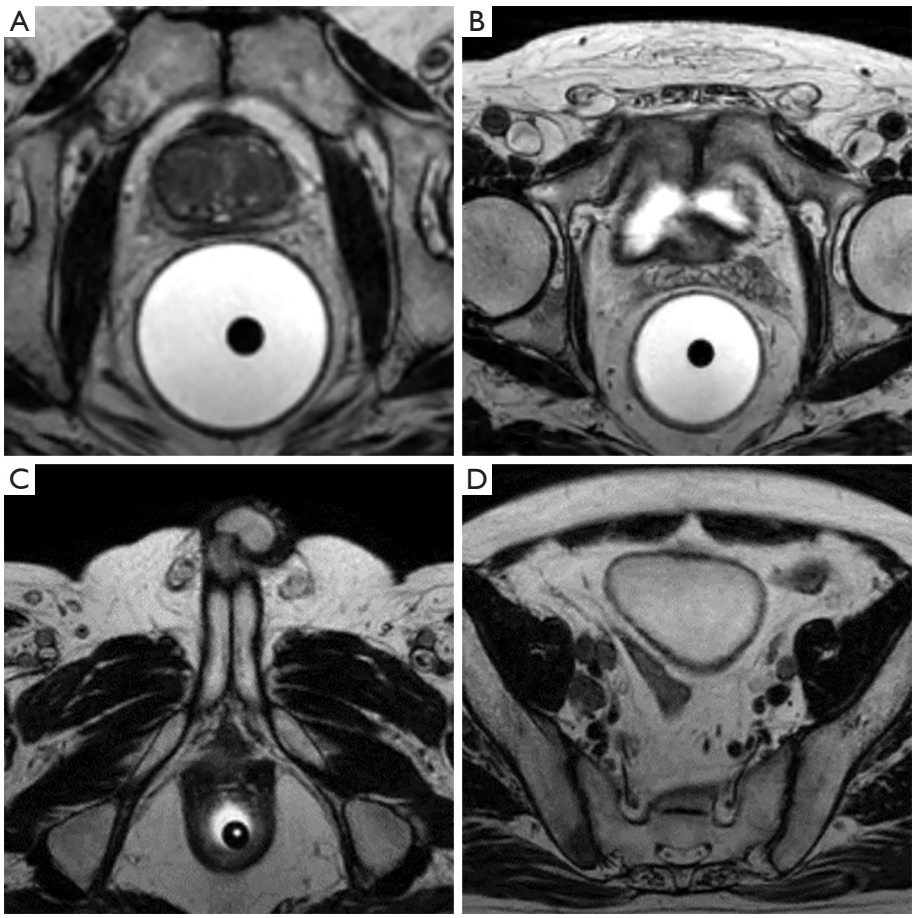

Figure 5 The anatomies in the T2-weighted MRgRT planning MRI: prostate (A) and various OARs of seminal vesicle (B), penis (C), bowel (D), and nerves (D). MRgRT, MR-guided radiotherapy; OARs, organs-at-risk.

planning is the preference of the 3D-T2W-TSE over the 2D-T2W-TSE sequence commonly used in the diagnostic MRI. The image contrast in 3D-T2W-TSE image is slightly different from, but rated equivalent to that in 2D-T2W-TSE images (59) due to the complicated flip angle modulation pattern in the long echo train implemented in the 3D-T2W-TSE sequence (60). Meanwhile, 3D-T2W-TSE is also more motion susceptible. But, their diagnostic performance in lesion detection is reported insignificantly different (59). It is postulated that 3D-T2W-TSE should perform better than 2D-T2W-TSE for anatomical delineation in the PCa MRgRT treatment planning, but such comparison is so far not yet reported in the literature.

For online MRI, both the daily MRI and the verification MRI are usually acquired using a built-in low-resolution 3D-T2W-TSE sequence with fixed imaging parameters (TE/TR =278/1,535 ms, echo-train-length =114, FOV =400 mm, acquisition voxel size =1.5×1.5×2.0 mm^3, duration =117 s) to balance the tradeoff between online adaptation efficiency and accuracy. Its spatial resolution is relatively lower than that in the planning MRI to save scan time, reducing the chance of patient position change, but acceptable for anatomical visualization to facilitate re-contouring and image registration.

Figure 6 depicts the T2W planning MRI acquired using a 3D-T2W-TSE sequence with an isotropic 1mm voxel size (upper row), and the T2W online MRI acquired using the fixed built-in 3D-T2W-TSE sequence (lower row), reformatted in the orthogonal views.

T1W MRI

T1W sequence with or without GBCA administration

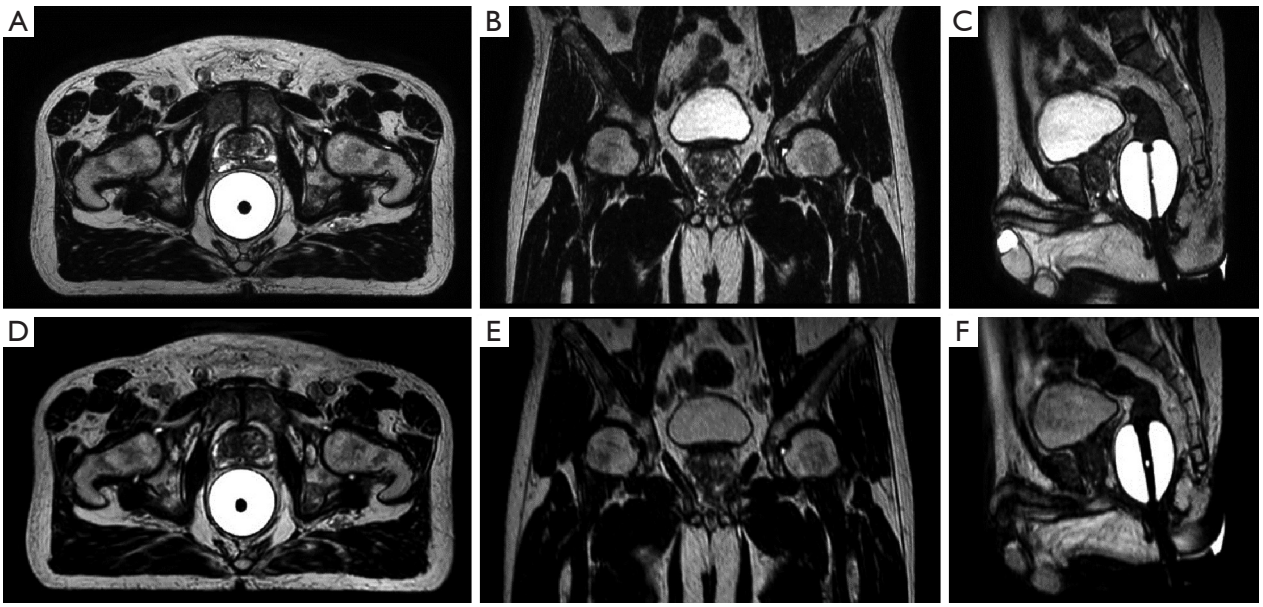

Figure 6 The T2W planning MRI acquired on a 1.5 T MR-simulator using a 3D-T2W-TSE sequence with an isotropic 1 mm voxel size (A-C), and the T2W online MRI acquired on a 1.5 T MR-LINAC using the fixed built-in 3D-T2W-TSE sequence with a voxel size of 1.5×1.5×2.0 mm^3 (D-F) in the orthogonal views. MR-LINAC, MRI and linear accelerator system; 3D-T2W-TSE, 3D T2-weighted turbo spin echo.

should be obtained in the diagnostic MRI as per PI-RADS, primarily to determine the presence of hemorrhage within the prostate and seminal vesicles, to delineate the gland outline, and to detect nodal and skeletal metastases (with post-contrast T1W) (48). In the MRgRT planning MRI, T1W sequence is often optional but not necessary for some reasons. First of all, the presence/absence of nodal and/or skeletal metastases as well as hemorrhage and their locations are usually the prior knowledge that has been obtained rather than the clinical question to be answered by the planning MRI. Second, T2W images might not be much inferior to T1W images for nodal or skeletal metastases visualization (if they are present), in particular in the absence of GBCA administration. In fact, it is well recognized that both T2W and T1W MRI has limited value in the diagnosis of lymph node metastases, mainly based on the nodal short axis measurement (61).

DWI

Like T2W MRI, DWI, acquired using a 2D single shot (SS) echo planar imaging (EPI) sequence, is a key component of mpMRI or bpMRI scan protocol in the diagnostic prostate MRI (12). High-b value DWI images (as per PI-RADS, "high b-value" means >1,400 sec/mm^2, could be acquired or calculated) and apparent diffusion coefficient (ADC) maps play a definitive role in the PI-RADS assessment of the peripheral zone (12). In contrast, for MRgRT planning MRI, DWI is currently optional or can even be omitted based on the fact of whole prostate irradiation in the current PCa MRgRT. But, DWI might be potentially valuable in the dose escalation to the dominant intra-prostatic lesions (DILs), particularly in the peripheral zone (62,63). In this scenario, DILs have to be additionally delineated from the whole prostate for extra dose prescription. However, severe image distortion and various artifacts in SS-EPI DWI present a critical challenge in the co-registration to other images in the MRgRT treatment planning.

DWI acquisition on a 1.5 T MR-LINAC is technically much more challenging than on a diagnostic MRI scanner due to its compromised gradient performance (25). A longer diffusion time (Δ) and thus a longer minimum echo time (TE) are needed for the same b-value. Along with the use of sub-optimal two 4-channel coils, these factors lead to the reduced DWI SNR on a 1.5 T MR-LINAC. Meanwhile, spatial dependent ADC values are noticed due to its split gradients design (25). The highest b-value of 500 s/mm^2 is recommended for ADC measurement on a 1.5 T MR-

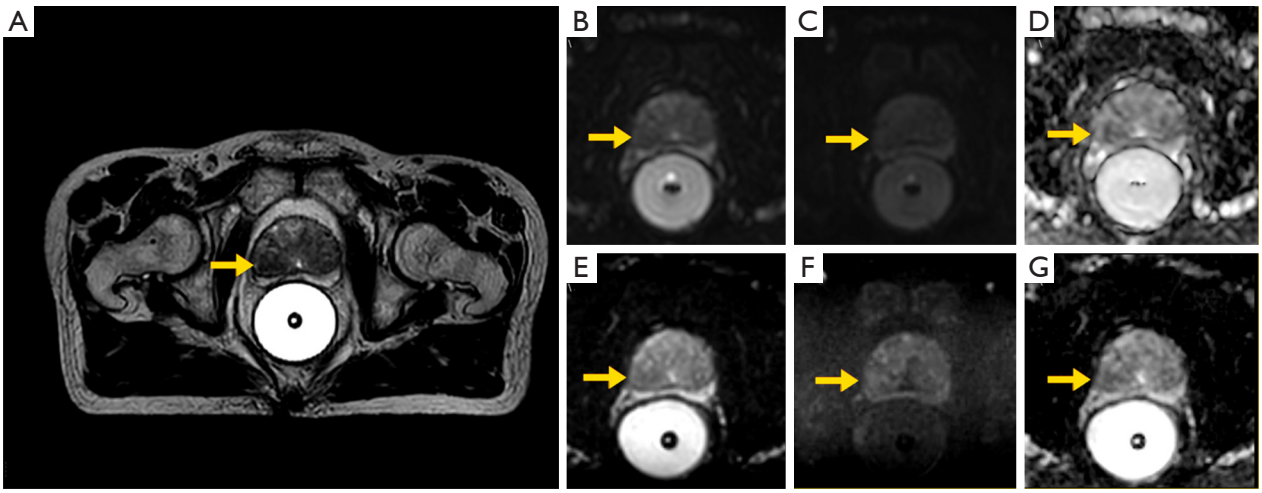

Figure 7 The prostate DWI images acquired on a 1.5 T MR-LINAC with the b-value of 0 and 500 s/mm^2 (B,C), and on a 1.5 T MR-sim with the b-value of 0 and 800 s/mm^2 (E,F). The corresponding ADC maps (D: MR-LINAC, G: MR-sim) and the T2W anatomical image (A) are also illustrated. The arrows correspond to the location of the prostate tumor. DWI, diffusion-weighted imaging; MR-LINAC, MRI and linear accelerator system; MR-sim, MR-simulator; ADC, apparent diffusion coefficient

LINAC, much lower than the PI-RADS recommended 800–1,000 s/mm^2 (25). High b-value (>1,400 sec/mm^2) DWI on a 1.5 T MR-LINAC has not been reported for clinical use in the literature, might have to be calculated rather than being acquired.

Figure 7 shows the prostate DWI images of a PCa MRgRT patients acquired on a 1.5 T MR-sim and a 1.5 T MR-LINAC.

DCE-MRI

DCE-MRI, normally acquired to obtain kinetic information of image intensity enhancement during and after the GBCA administration using a rapid 3D gradient echo sequence, provides modest added value for PI-RADS assessment over the combination of T2W and DWI in the mpMRI protocol (44). But, in the MRgRT planning MRI, it might be omitted provided that such information has been obtained by the diagnostic MRI. It is of little added value of either DCE-MRI or T1W for anatomical delineation over T2W. Other issues related to the use of DCE-MRI are increased cost, complex logistics, longer scan time, and potential GBCA safety events. For MRgRT online MRI, DCE-MRI should not be conducted for the similar reasons.

Proton MR spectroscopy (MRS)

Proton MRS, a previous component of mpMRI, has no longer been included in the latest version of PI-RADS (49) due to its unclear diagnostic benefit (12). In addition, proton MRS also has the limitations like high complexity, low availability, long acquisition time but low reliability, the need for dedicated software and interpretation by experienced radiologists. It has no clinical role in the MRgRT MRI of prostate cancer at present.

Balanced steady state free precession (bSSFP)

The bSSFP sequence is a useful sequence for MRgRT online MRI. This sequence provides distinctive T2/T1 image contrast and has the highest SNR efficiency in all gradient echo sequences (64). bSSFP is the dominant workhorse sequence on the 0.35 T MR-LINAC to obtain somewhat T2-like image contrast in that 3D-TSE sequence is technically challenging to implement on the low-field MR-LINAC. The bSSFP acquisition can be conducted with a very short repetition time (TR), so can achieve very high temporal resolution of ~200 ms/slice in MRgRT. A major role of bSSFP in MRgRT (both 1.5 T and 0.35 T) is for motion management, in particular for online MRI during radiation dose delivery, in which bSSFP images of a few orthogonal slices is continuously acquired in real time, named orthogonal CINE (65), to capture the anatomical motions, so as to facilitate treatment gating and tracking (currently only at 0.35 T). *Figure 8* shows the orthogonal bSSFP CINE images acquired on a 1.5 T MR-LINAC.

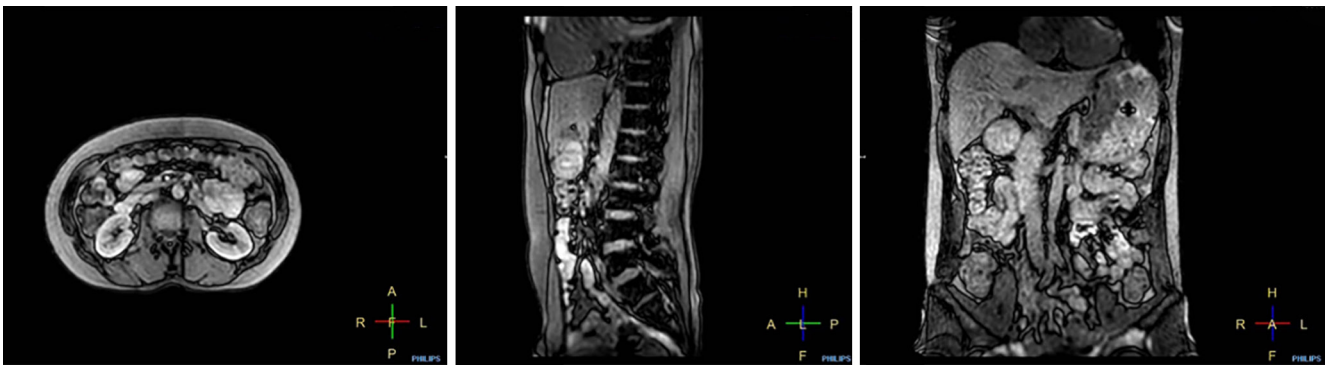

Figure 8 The orthogonal bSSFP CINE MRI of a healthy volunteer with a temporal resolution of 200 milliseconds (per image) acquired on a 1.5 T integrated MR-LINAC. bSSFP, balanced steady state free precession; MR-LINAC, MRI and linear accelerator system.

Since respiratory motion is not pronounced in the pelvis, bSSFP is often optionally acquired during dose delivery in the 1.5 T PCa MRgRT.

Other MRI acquisition techniques

There are other potentially useful but currently optional sequences for PCa MRgRT. For example, T2*-weighted MRI acquired using gradient echo sequences with long TE was proposed for better delineation of prostate capsule in the RT treatment planning (66,67). Dixon imaging can be used to generate synthetic CT images for dose calculation so as to omit planning CT and achieve the MR-only workflow of MRgRT (68,69), as shown in *Figure 9*. It is worth noting that these sequences are currently not used or not yet implemented on the MR-LINAC. Many other MRI techniques proposed for diagnostic prostate MRI, such as chemical exchange saturation transfer (CEST) (70), blood-oxygen-level-dependent (BOLD) MRI (71), ultrasmall superparamagnetic iron oxide (USPIO) particle MRI (72), intravoxel incoherent motion (IVIM) (73), hyperpolarized 13C-pyruvate MRI (74), have not yet found their clear roles in the PCa MRgRT.

Limitation and future development of MRI in PCa MRgRT

MRgRT presents a revolutionary solution on the future radiotherapy of PCa treatment, preliminary clinical outcomes of PCa MRgRT are emerging (75-79). It is postulated that the clinical outcome of MRgRT should greatly benefit from the utilization of both anatomical and functional MRI techniques. In addition, fast MRI techniques can also greatly reduce the duration and increase the efficiency of MRgRT, so as to justify its cost effectiveness value (80).

Although knowledge and experience of PCa MRgRT has developed rapidly with the faster pace of worldwide MR-LINAC installation and clinical deployment in recent years, the current MRgRT still has some limitations and challenges to be overcome to realize its maximal potentials and fulfill its clinical promises (80,81).

Regarding the planning MRI in PCa MRgRT, there is still no well recognized or standardized scan protocol. It is not uncommon that the planning MRI duplicates the mpMRI, thus providing redundant information with the diagnostic MRI to some degrees. But this redundant information might have limited added value for anatomical delineation in MRgRT planning. Meanwhile, the use of 2D-TSE in MRgRT planning MRI might be sub-optimal due to its highly anisotropic voxel size, slightly poorer distortion profile and lower scan efficiency.

We consider that the single-parametric 3D-T2W-TSE MRI acquired in the treatment position should be able to meet the minimal requirement for anatomical delineation in PCa MRgRT treatment planning, in particular when recent diagnostic mpMRI is available to obtain the prior knowledge such as tumor location, size, EPE and lymph node metastases. The limitation of individual PCa tumor visualization on the single-parametric T2W planning MRI should be recognized, in particular for the consideration of the highest field strength of 1.5 T for an MR-LINAC and the sub-optimal RF coils. But this issue might not be on the highest priority to address or overcome as long as the whole prostate irradiation is applied in the MRgRT. A 3D-T2W-TSE acquisition with high spatial resolution, e.g., ≤1 mm

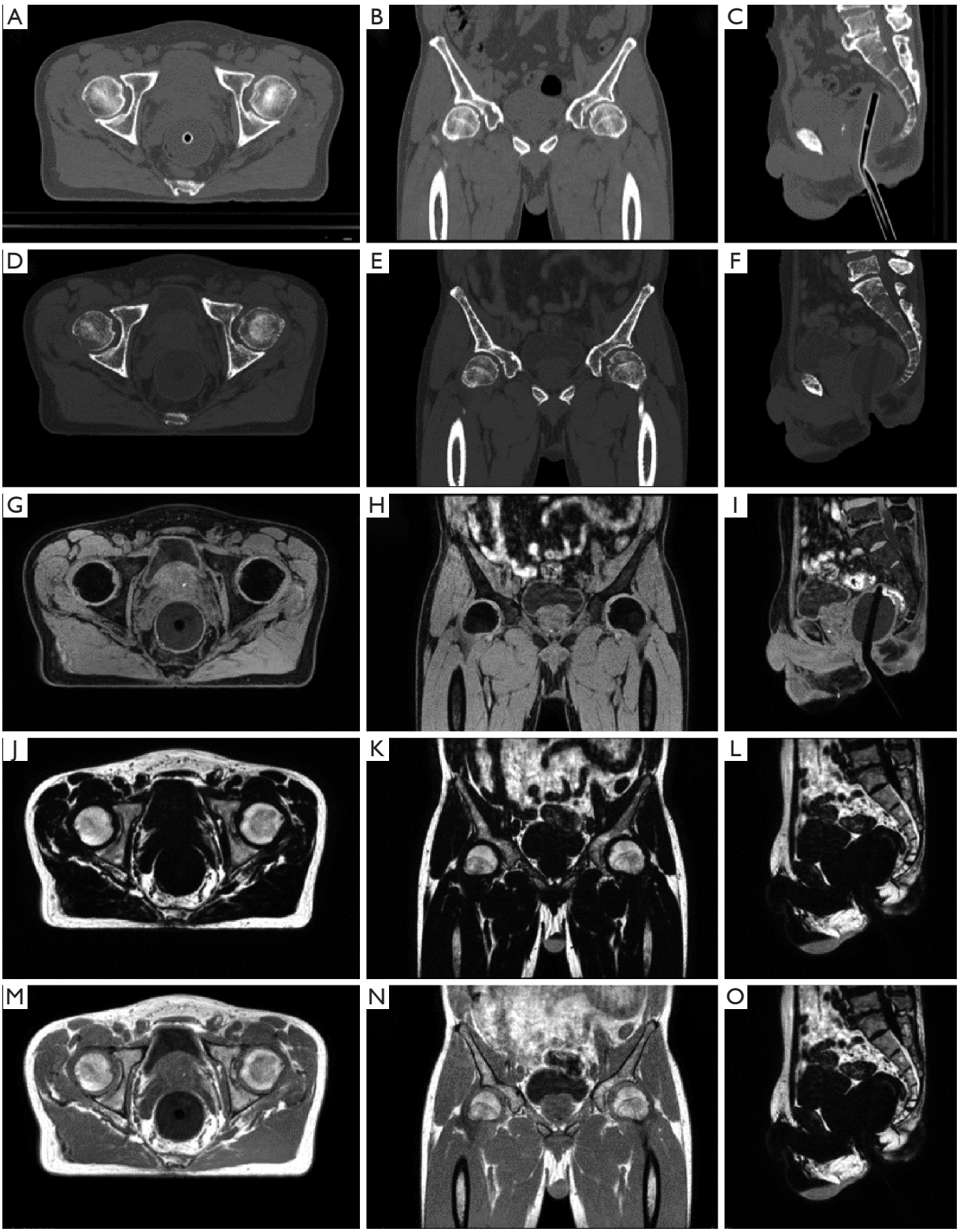

Figure 9 Dixon imaging for synthetic CT generation provides a potential solution of MR-only workflow in the future prostate cancer MRgRT. (A-C) True planning CT; (D-F) synthetic CT generated based on Dixon MRI images; (G-I) Dixon water-only images; (J-L) Dixon fat-only images; (M-O) original in-phase images. MRgRT, MR-guided radiotherapy.

isotropic voxel size, in a large image volume could be time consuming, even with a very long echo-train-length. Another potential concern is the image burring induced by the long echo train duration in 3D-T2W-TSE that might compromise fine structure delineation or DIL definition for dose boosting. In our observation, the blurring is very minor in the online 3D-T2W-TSE images. So far there has been no study investigated its influence on delineation or registration accuracy in MRgRT. Compressed sensing (CS) should be helpful to further accelerate 3D-T2W-TSE acquisition and reduce its echo train duration compared with the currently widely applied parallel imaging techniques (82,83).

The clinical value of DWI for DIL dose escalation is yet to be explored. Some technical challenges are its low spatial resolution, pronounced distortion and other artifacts, and poor SNR at high b-values. Regarding geometric fidelity, non-EPI based DWI might have potentials on better image co-registration accuracy so as to improve treatment precision, but there are still other problems to overcome (84). In long term, development of 3D distortion-free high-resolution DWI should be definitely useful in the future MRgRT, but requires enormous research efforts (85,86). The value of DCE-MRI is currently at least uncertain, and probably unfavorable in the PCa MRgRT planning MRI as it provides limited added value of anatomical delineation to T2W MRI. But, quantitative DCE-MRI and its kinetic parameters might provide potential values in the future MRgRT (87).

Dixon MRI based on 3D T1W gradient echo sequence has been commercialized for synthetic CT generation in the pelvis on MR-sims, but not yet on MR-LINACs, aiming to implement an MR-only clinical workflow in the PCa MRgRT. This MR-only workflow not only omits the planning CT to simplify the workflow, but also potentially improves the precision of PCa MRgRT by completely eliminating the planning CT-MRI co-registration error. But this technique still subjects to some pitfalls and limitations, so needs to be further improved (68,69). In addition, extra acquisition is required so prolongs the scan time, while 3D-T1W-Dixon itself has limited added value in anatomical delineation. An attractive solution would be the deep learning based synthetic CT generation from the single 3D-T2W-TSE, the pivotal sequence in the PCa MRgRT (88,89).

In contrast to the heterogeneous planning MRI protocols in the PCa MRgRT, the protocol of online MRI is highly consistent. Both daily MRI and verification MRI in the online MRI also rely heavily on 3D-T2W-TSE sequence, but whose spatial resolution is lower than that in the planning MRI to reduce the chance of patient positional change. Compressed sensing should be also useful for online 3D-T2W-TSE acquisition. There could be two approaches in the CS implementation, as illustrated in *Figure 10*. One is to increase spatial resolution within the similar scan time so as to potentially improve adaptation accuracy and precision. The other is to remain the image spatial resolution and quality, but with much shorter scan time to increase adaptation efficiency. But it is worth noting that the short CS reconstruction time is critical for the online MRI since these images are used for the immediate prospective viewing rather than the offline retrospective viewing. In addition, it would be helpful if synthetic CT could be generated from the 3D-T2W-TSE images to facilitate more accurate and efficient online dose calculation and treatment adaptation.

Online real-time motion MRI during beam-on time is a key advantage of MRgRT over conventional IGRTs. But, this advantage is yet to be fully realized because the current real-time motion MRI, i.e., the orthogonal bSSFP CINE MRI, on the MR-LINAC has many technical limitations to facilitate motion monitoring, dose delivery gating and tracking (65). First, the orthogonal bSSFP CINE MRI can only acquire images of very few slices, usually 1–3 slices. Otherwise, its temporal resolution, which is inversely proportional to the number of slices, will be much sacrificed. Moreover, the orthogonal bSSFP cine MRI cannot provide volumetric motion information of the target tumors and other anatomies in interests, but only motion in a few discrete slices. The orthogonal CINE MRI also associates with the dark banding artifact during repetitive acquisition, regardless of sequence type. These dark bands have the line-width equal to the prescribed slice thickness and intersect at the target anatomy.

The future online motion MRI for MRgRT, not only limited to PCa MRgRT, should ideally be able to provide volumetric motion information (with reasonably high spatial resolution) in the anatomies in real time to guide dose delivery (90,91). It is technically challenging, but definitely deserves investigation. Current 3D MRI sequences might barely achieve the volumetric temporal resolution in the level of several hundred milliseconds, which is minimally acceptable for respiratory motion tracking according to the Nyquist sampling theorem (92). But, one critical issue is its slow image reconstruction, causing the severe latency in image viewing, not to mention interacting with LINAC for real-time gating or tracking. Research efforts are being

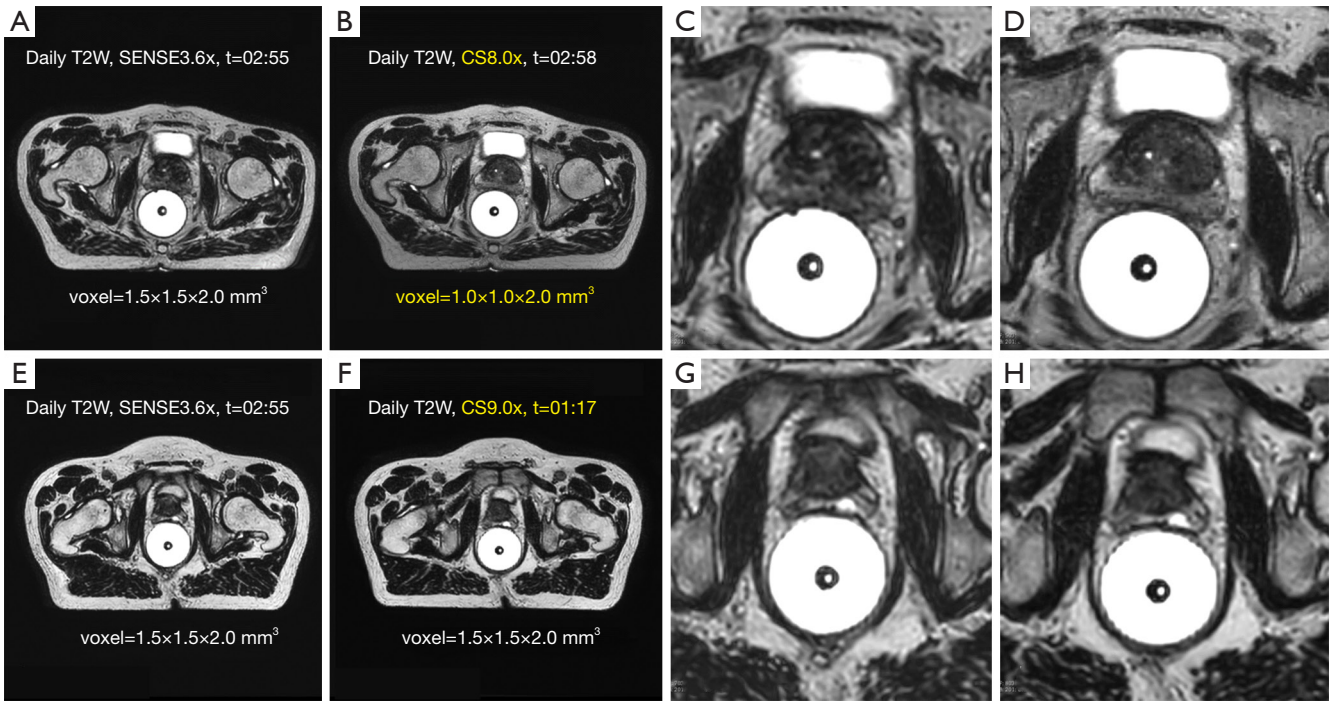

Figure 10 The application of CS for online 3D-T2W-TSE acquisition. Approach one: (A,C) the daily MRI images acquired using the built-in 3D-T2W-TSE sequence with a 3.6-fold sensitivity encoding (SENSE) acceleration; (B,D) the 8-fold CS accelerated 3D-T2W-TSE images with much higher spatial resolution but similar scan time. Approach two: (E,G) the daily MRI images acquired using the built-in 3D-T2W-TSE sequence with a 3.6-fold sensitivity encoding (SENSE) acceleration; (F,H) the 9-fold CS accelerated 3D-T2W-TSE images with the same spatial resolution but much shorter scan time. CS, compressed sensing; 3D-T2W-TSE, 3D T2-weighted turbo spin echo.

actively made on tackling this issue (93-96).

In recent years, deep learning is one of the fastest-growing fields in artificial intelligence, and has been actively explored and widely applied to many medical domains including medical imaging and radiotherapy (97,98). There is no doubt that deep learning is playing an increasingly important role in many aspects of MRgRT. Regarding MRI acquisition in PCa MRgRT, deep learning can greatly further accelerate acquisition by learning spatial and/or temporal dependencies of image appearance from the highly under sampled MRI k-space data, and outperforms parallel imaging and compressed sensing (99). Deep learning has been demonstrated to technically enable real-time image reconstruction and motion estimation for MRgRT (100). Furthermore, deep learning also has great potentials in multi-sequence or multi-model image synthesis (101) beyond synthetic CT generation, for the future MRgRT, including but not limited to PCa.

It is also recognized that the current MRI acquisition in PCa MRgRT are mostly anatomical sequences. Functional MRI techniques are now playing a very limited role in either planning MRI or online MRI for PCa MRgRT, although they have been vastly investigated for prostate cancer diagnosis, treatment prediction or treatment evaluation (71-74). Despite that, we believe that functional MRI could also play a bigger role in the future PCa MRgRT for both treatment planning and online treatment adaptation based on the tumor (functional or molecular rather than anatomical) property and its inter-fractional change that might be only detectable by functional MRI.

There is a long way ahead to establish the well acknowledged, standardized and optimized MRI acquisition protocol in PCa MRgRT. But, on the other hand, it is also important to establish image quality criteria for these images dedicatedly acquired for PCa MRgRT. The Prostate Imaging Quality (PI-QUAL) score, which assesses the mpMRI quality against a set of objective criteria together with criteria obtained from the image, has been proposed for diagnostic prostate MRI to make clinicians more confident in using the mpMRI to determine patient care

(102,103). As the MRI acquisition in PCa MRgRT has substantially different clinical purposes from mpMRI, PI-QUAL score might not be suitable or directly applicable for PCa MRgRT. But, a dedicated image quality appraisal system for PCa MRgRT is definitely desirable and deserves future exploration.

Study limitation

This narrative review associates with some limitations. It is illustrative rather than exhaustive. The literature search yields a huge number of publications, but most of them are not directly or closely related to MRI acquisition for PCa MRgRT. Many of them have to be excluded by subjective study selection, which might introduce potential bias. Since there is no well recognized consensus on the optimal patient selection for PCa MRgRT, this review only represents a general typical strategy for MRI acquisition in PCa MRgRT, but does not specify to different types of PCa patient in different clinical scenarios, e.g., recurrent PCa patients for re-irradiation or post-surgery irradiation by MRgRT. Current MRI acquisition protocols in MRgRT are introduced or proposed based mainly on technical rationale or feasibility, while their correlation with major clinical endpoints in MRgRT is largely unknown. More clinical evidences should be established to justify and refine these protocols in MRgRT, just like those done for diagnostic mpMRI in the PI-RADS development. Due to the lack of strong consensus on MRI acquisition that could be synthesized from literature appraisal, some interpretations in this review might be subjective based on our own clinical and research experiences in MRgRT, which should be considered to be reference instead of clinical suggestion or recommendation. Finally, knowledge on MRI acquisition in this review is subject to change and update with the fast evolution of MRgRT in its technical development and clinical application.

Conclusions

This study provides a comprehensive overview of MRI acquisition in the current clinical workflow of PCa MRgRT, from treatment planning to online treatment guidance, which is substantially different from that in the diagnostic prostate MRI and has special considerations for fulfilling radiotherapy purposes. In the treatment planning, there is currently no well recognized or standardized MRI acquisition protocol. T2W MRI acquired in the treatment position using 3D TSE sequence is pivotal for whole prostate and other OAR delineation. In the daily plan adaptation, 3D-T2W-TSE and bSSFP are dominant for high field and low field MRgRT, respectively. These acquisition protocols are highly consistent, but might be further optimized in the future development. 2D orthogonal CINE acquisition represents the current MRI acquisition approach on MR-LINAC for real-time motion monitoring, treatment gating and/or tracking, but subjects to some limitations. DWI should be useful to define dominant intra-prostatic lesion for dose escalation in combination with T2W MRI, but its acquisition is technically challenging on MR-LINAC. The future development of MRI acquisition in PCa MRgRT should greatly benefit from fast imaging sequences and novel reconstruction techniques. MRI-only workflow based on MRI derived synthetic CT, not only in treatment planning but in daily adaptation, is attractive and deserves further exploration. Anatomical MRI plays the central role in the current practice of MRI acquisition for PCa MRgRT. The potentials of functional MRI techniques for the future PCa MRgRT are to be explored.

Acknowledgments

Funding: This study was supported by hospital research project REC-2019-09.

Footnote

Reporting Checklist: The authors have completed the Narrative Review Checklist. Available at https://dx.doi.org/10.21037/qims-21-697

Conflicts of Interest: All authors have completed the ICMJE uniform disclosure form (available at https://dx.doi.org/10.21037/qims-21-697). JY reports that he received honoraria for a lecture from Philips Healthcare in 2019. JY serves as an unpaid editorial board member of *Quantitative Imaging in Medicine and Surgery*. The other authors have no conflicts of interest to declare.

Ethical Statement: The authors are accountable for all aspects of the work in ensuring that questions related to the accuracy or integrity of any part of the work are appropriately investigated and resolved.

References

1. Rawla P. Epidemiology of Prostate Cancer. World J Oncol 2019;10:63-89.
2. Litwin MS, Tan HJ. The Diagnosis and Treatment of Prostate Cancer: A Review. JAMA 2017;317:2532-42.
3. Dearnaley D, Syndikus I, Mossop H, Khoo V, Birtle A, Bloomfield D, et al. Conventional versus hypofractionated high-dose intensity-modulated radiotherapy for prostate cancer: 5-year outcomes of the randomised, non-inferiority, phase 3 CHHiP trial. Lancet Oncol 2016;17:1047-60.
4. de Vries KC, Wortel RC, Oomen-de Hoop E, Heemsbergen WD, Pos FJ, Incrocci L. Hyprofractionated Versus Conventionally Fractionated Radiation Therapy for Patients with Intermediate- or High-Risk, Localized, Prostate Cancer: 7-Year Outcomes From the Randomized, Multicenter, Open-Label, Phase 3 HYPRO Trial. Int J Radiat Oncol Biol Phys 2020;106:108-15.
5. Lagendijk JJ, Raaymakers BW, Van den Berg CA, Moerland MA, Philippens ME, van Vulpen M. MR guidance in radiotherapy. Phys Med Biol 2014;59:R349-69.
6. Kupelian P, Sonke JJ. Magnetic resonance-guided adaptive radiotherapy: a solution to the future. Semin Radiat Oncol 2014;24:227-32.
7. Henke LE, Contreras JA, Green OL, Cai B, Kim H, Roach MC, et al. Magnetic Resonance Image-Guided Radiotherapy (MRIgRT): A 4.5-Year Clinical Experience. Clin Oncol (R Coll Radiol) 2018;30:720-7.
8. Lagendijk JJ, Raaymakers BW, Raaijmakers AJ, Overweg J, Brown KJ, Kerkhof EM, van der Put RW, Hårdemark B, van Vulpen M, van der Heide UA. MRI/linac integration. Radiother Oncol 2008;86:25-9.
9. Lagendijk JJ, Raaymakers BW, van Vulpen M. The magnetic resonance imaging-linac system. Semin Radiat Oncol 2014;24:207-9.
10. Mutic S, Dempsey JF. The ViewRay system: magnetic resonance-guided and controlled radiotherapy. Semin Radiat Oncol 2014;24:196-9.
11. Jones KM, Michel KA, Bankson JA, Fuller CD, Klopp AH, Venkatesan AM. Emerging Magnetic Resonance Imaging Technologies for Radiation Therapy Planning and Response Assessment. Int J Radiat Oncol Biol Phys 2018;101:1046-56.
12. Stabile A, Giganti F, Rosenkrantz AB, Taneja SS, Villeirs G, Gill IS, Allen C, Emberton M, Moore CM, Kasivisvanathan V. Multiparametric MRI for prostate cancer diagnosis: current status and future directions. Nat Rev Urol 2020;17:41-61.
13. Turkbey B, Rosenkrantz AB, Haider MA, Padhani AR, Villeirs G, Macura KJ, Tempany CM, Choyke PL, Cornud F, Margolis DJ, Thoeny HC, Verma S, Barentsz J, Weinreb JC. Prostate Imaging Reporting and Data System Version 2.1: 2019 Update of Prostate Imaging Reporting and Data System Version 2. Eur Urol 2019;76:340-51.
14. Weinreb JC, Barentsz JO, Choyke PL, Cornud F, Haider MA, Macura KJ, Margolis D, Schnall MD, Shtern F, Tempany CM, Thoeny HC, Verma S. PI-RADS Prostate Imaging - Reporting and Data System: 2015, Version 2. Eur Urol 2016;69:16-40.
15. Dinh CV, Steenbergen P, Ghobadi G, Heijmink SW, Pos FJ, Haustermans K, van der Heide UA. Magnetic resonance imaging for prostate cancer radiotherapy. Phys Med 2016;32:446-51.
16. Schmidt MA, Payne GS. Radiotherapy planning using MRI. Phys Med Biol 2015;60:R323-61.
17. Paulson ES, Erickson B, Schultz C, Allen Li X. Comprehensive MRI simulation methodology using a dedicated MRI scanner in radiation oncology for external beam radiation treatment planning. Med Phys 2015;42:28-39.
18. Devic S. MRI simulation for radiotherapy treatment planning. Med Phys 2012;39:6701-11.
19. Glide-Hurst CK, Paulson ES, McGee K, Tyagi N, Hu Y, Balter J, Bayouth J. Task group 284 report: magnetic resonance imaging simulation in radiotherapy: considerations for clinical implementation, optimization, and quality assurance. Med Phys 2021;48:e636-70.
20. Wong OL, Yuan J, Yu SK, Cheung KY. Image quality assessment of a 1.5T dedicated magnetic resonance-simulator for radiotherapy with a flexible radio frequency coil setting using the standard American College of Radiology magnetic resonance imaging phantom test. Quant Imaging Med Surg 2017;7:205-14.
21. Mekiš V, Žager Marciuš V, Rogina D, Dolenc L, Mekiš N. Comparison of treatment position with mask immobilization and standard diagnostic setup in intracranial MRI radiotherapy simulation. Strahlenther

Onkol 2021;197:614-21.
22. Raaymakers BW, Jürgenliemk-Schulz IM, Bol GH, Glitzner M, Kotte ANTJ, van Asselen B, et al. First patients treated with a 1.5 T MRI-Linac: clinical proof of concept of a high-precision, high-field MRI guided radiotherapy treatment. Phys Med Biol 2017;62:L41-50.
23. Winkel D, Bol GH, Kroon PS, van Asselen B, Hackett SS, Werensteijn-Honingh AM, Intven MPW, Eppinga WSC, Tijssen RHN, Kerkmeijer LGW, de Boer HCJ, Mook S, Meijer GJ, Hes J, Willemsen-Bosman M, de Groot-van Breugel EN, Jürgenliemk-Schulz IM, Raaymakers BW. Adaptive radiotherapy: The Elekta Unity MR-linac concept. Clin Transl Radiat Oncol 2019;18:54-9.
24. Tijssen RHN, Philippens MEP, Paulson ES, Glitzner M, Chugh B, Wetscherek A, Dubec M, Wang J, van der Heide UA. MRI commissioning of 1.5T MR-linac systems - a multi-institutional study. Radiother Oncol 2019;132:114-20.
25. Kooreman ES, van Houdt PJ, Keesman R, Pos FJ, van Pelt VWJ, Nowee ME, Wetscherek A, Tijssen RHN, Philippens MEP, Thorwarth D, Wang J, Shukla-Dave A, Hall WA, Paulson ES, van der Heide UA. ADC measurements on the Unity MR-linac - A recommendation on behalf of the Elekta Unity MR-linac consortium. Radiother Oncol 2020;153:106-13.
26. Tocco BR, Kishan AU, Ma TM, Kerkmeijer LGW, Tree AC. MR-Guided Radiotherapy for Prostate Cancer. Front Oncol 2020;10:616291.
27. Giganti F, Kirkham A, Allen C, Punwani S, Orczyk C, Emberton M, Moore CM. Update on Multiparametric Prostate MRI During Active Surveillance: Current and Future Trends and Role of the PRECISE Recommendations. AJR Am J Roentgenol 2021;216:943-51.
28. Dirix P, Haustermans K, Vandecaveye V. The value of magnetic resonance imaging for radiotherapy planning. Semin Radiat Oncol 2014;24:151-9.
29. Kashani R, Olsen JR. Magnetic Resonance Imaging for Target Delineation and Daily Treatment Modification. Semin Radiat Oncol 2018;28:178-84.
30. de Muinck Keizer DM, Kerkmeijer LGW, Willigenburg T, van Lier ALHMW, Hartogh MDD, van der Voort van Zyp JRN, de Groot-van Breugel EN, Raaymakers BW, Lagendijk JJW, de Boer JCJ. Prostate intrafraction motion during the preparation and delivery of MR-guided radiotherapy sessions on a 1.5T MR-Linac. Radiother Oncol 2020;151:88-94.
31. Paganelli C, Whelan B, Peroni M, Summers P, Fast M, van de Lindt T, McClelland J, Eiben B, Keall P, Lomax T, Riboldi M, Baroni G. MRI-guidance for motion management in external beam radiotherapy: current status and future challenges. Phys Med Biol 2018;63:22TR03.
32. Lee YK, Bollet M, Charles-Edwards G, Flower MA, Leach MO, McNair H, Moore E, Rowbottom C, Webb S. Radiotherapy treatment planning of prostate cancer using magnetic resonance imaging alone. Radiother Oncol 2003;66:203-16.
33. Debois M, Oyen R, Maes F, Verswijvel G, Gatti G, Bosmans H, Feron M, Bellon E, Kutcher G, Van Poppel H, Vanuytsel L. The contribution of magnetic resonance imaging to the three-dimensional treatment planning of localized prostate cancer. Int J Radiat Oncol Biol Phys 1999;45:857-65.
34. Paulson ES, Crijns SP, Keller BM, Wang J, Schmidt MA, Coutts G, van der Heide UA. Consensus opinion on MRI simulation for external beam radiation treatment planning. Radiother Oncol 2016;121:187-92.
35. Metcalfe P, Liney GP, Holloway L, Walker A, Barton M, Delaney GP, Vinod S, Tome W. The potential for an enhanced role for MRI in radiation-therapy treatment planning. Technol Cancer Res Treat 2013;12:429-46.
36. Tree AC, Huddart R, Choudhury A. Magnetic Resonance-guided Radiotherapy - Can We Justify More Expensive Technology? Clin Oncol (R Coll Radiol) 2018;30:677-9.
37. Kooreman ES, van Houdt PJ, Nowee ME, van Pelt VWJ, Tijssen RHN, Paulson ES, Gurney-Champion OJ, Wang J, Koetsveld F, van Buuren LD, Ter Beek LC, van der Heide UA. Feasibility and accuracy of quantitative imaging on a 1.5 T MR-linear accelerator. Radiother Oncol 2019;133:156-62.
38. Pinkawa M, Asadpour B, Gagel B, Piroth MD, Holy R, Eble MJ. Prostate position variability and dose-volume histograms in radiotherapy for prostate cancer with full and empty bladder. Int J Radiat Oncol Biol Phys 2006;64:856-61.
39. Maggio A, Gabriele D, Garibaldi E, Bresciani S, Delmastro E, Di Dia A, Miranti A, Poli M, Varetto T, Stasi M, Gabriele P. Impact of a rectal and bladder preparation protocol on prostate cancer outcome in patients treated with external beam radiotherapy. Strahlenther Onkol 2017;193:722-32.
40. Gawlitza J, Reiss-Zimmermann M, Thörmer G, Schaudinn A, Linder N, Garnov N, Horn LC, Minh DH, Ganzer R, Stolzenburg JU, Kahn T, Moche M, Busse H. Impact of the use of an endorectal coil for 3 T prostate MRI on image quality and cancer detection rate. Sci Rep 2017;7:40640.

41. Smeenk RJ, Louwe RJ, Langen KM, Shah AP, Kupelian PA, van Lin EN, Kaanders JH. An endorectal balloon reduces intrafraction prostate motion during radiotherapy. Int J Radiat Oncol Biol Phys 2012;83:661-9.
42. Alongi F, Rigo M, Figlia V, Cuccia F, Giaj-Levra N, Nicosia L, Ricchetti F, Vitale C, Sicignano G, De Simone A, Naccarato S, Ruggieri R, Mazzola R. Rectal spacer hydrogel in 1.5T MR-guided and daily adapted SBRT for prostate cancer: dosimetric analysis and preliminary patient-reported outcomes. Br J Radiol 2021;94:20200848.
43. Cuccia F, Mazzola R, Nicosia L, Figlia V, Giaj-Levra N, Ricchetti F, Rigo M, Vitale C, Mantoan B, De Simone A, Sicignano G, Ruggieri R, Cavalleri S, Alongi F. Impact of hydrogel peri-rectal spacer insertion on prostate gland intra-fraction motion during 1.5 T MR-guided stereotactic body radiotherapy. Radiat Oncol 2020 22;15:178.
44. Berman RM, Brown AM, Chang SD, Sankineni S, Kadakia M, Wood BJ, Pinto PA, Choyke PL, Turkbey B. DCE MRI of prostate cancer. Abdom Radiol (NY) 2016;41:844-53.
45. Walker A, Liney G, Metcalfe P, Holloway L. MRI distortion: considerations for MRI based radiotherapy treatment planning. Australas Phys Eng Sci Med 2014;37:103-13.
46. Weygand J, Fuller CD, Ibbott GS, Mohamed AS, Ding Y, Yang J, Hwang KP, Wang J. Spatial Precision in Magnetic Resonance Imaging-Guided Radiation Therapy: The Role of Geometric Distortion. Int J Radiat Oncol Biol Phys 2016;95:1304-16.
47. Seibert TM, White NS, Kim GY, Moiseenko V, McDonald CR, Farid N, Bartsch H, Kuperman J, Karunamuni R, Marshall D, Holland D, Sanghvi P, Simpson DR, Mundt AJ, Dale AM, Hattangadi-Gluth JA. Distortion inherent to magnetic resonance imaging can lead to geometric miss in radiosurgery planning. Pract Radiat Oncol 2016;6:e319-28.
48. Purysko AS, Baroni RH, Giganti F, Costa D, Renard-Penna R, Kim CK, Raman SS. PI-RADS Version 2.1: A Critical Review, From the AJR Special Series on Radiology Reporting and Data Systems. AJR Am J Roentgenol 2021;216:20-32.
49. Hoeks CM, Barentsz JO, Hambrock T, Yakar D, Somford DM, Heijmink SW, Scheenen TW, Vos PC, Huisman H, van Oort IM, Witjes JA, Heerschap A, Fütterer JJ. Prostate cancer: multiparametric MR imaging for detection, localization, and staging. Radiology 2011;261:46-66.
50. Padhani AR, Barentsz J, Villeirs G, Rosenkrantz AB, Margolis DJ, Turkbey B, Thoeny HC, Cornud F, Haider MA, Macura KJ, Tempany CM, Verma S, Weinreb JC. PI-RADS Steering Committee: The PI-RADS Multiparametric MRI and MRI-directed Biopsy Pathway. Radiology 2019;292:464-74.
51. Kuhl CK, Bruhn R, Krämer N, Nebelung S, Heidenreich A, Schrading S. Abbreviated Biparametric Prostate MR Imaging in Men with Elevated Prostate-specific Antigen. Radiology 2017;285:493-505.
52. Niu XK, Chen XH, Chen ZF, Chen L, Li J, Peng T. Diagnostic Performance of Biparametric MRI for Detection of Prostate Cancer: A Systematic Review and Meta-Analysis. AJR Am J Roentgenol 2018;211:369-78.
53. Sherrer RL, Glaser ZA, Gordetsky JB, Nix JW, Porter KK, Rais-Bahrami S. Comparison of biparametric MRI to full multiparametric MRI for detection of clinically significant prostate cancer. Prostate Cancer Prostatic Dis 2019;22:331-6.
54. Villeirs GM, De Meerleer GO. Magnetic resonance imaging (MRI) anatomy of the prostate and application of MRI in radiotherapy planning. Eur J Radiol 2007;63:361-8.
55. van Schie MA, Dinh CV, Houdt PJV, Pos FJ, Heijmink SWTJP, Kerkmeijer LGW, Kotte ANTJ, Oyen R, Haustermans K, van der Heide UA. Contouring of prostate tumors on multiparametric MRI: Evaluation of clinical delineations in a multicenter radiotherapy trial. Radiother Oncol 2018;128:321-6.
56. Salembier C, Villeirs G, De Bari B, Hoskin P, Pieters BR, Van Vulpen M, Khoo V, Henry A, Bossi A, De Meerleer G, Fonteyne V. ESTRO ACROP consensus guideline on CT- and MRI-based target volume delineation for primary radiation therapy of localized prostate cancer. Radiother Oncol 2018;127:49-61.
57. Johnson DC, Raman SS, Mirak SA, Kwan L, Bajgiran AM, Hsu W, Maehara CK, Ahuja P, Faiena I, Pooli A, Salmasi A, Sisk A, Felker ER, Lu DSK, Reiter RE. Detection of Individual Prostate Cancer Foci via Multiparametric Magnetic Resonance Imaging. Eur Urol 2019;75:712-20.
58. von Hardenberg J, Borkowetz A, Siegel F, Kornienko K, Westhoff N, Jordan TB, Hoffmann M, Drerup M, Lieb V, Taymoorian K, Schostak M, Ganzer R, Höfner T, Cash H, Bruendl J; GESRU Academics Prostate Cancer Group in cooperation with the Working Group of Focal and Microtherapy of the German Society of Urology (DGU). Potential Candidates for Focal Therapy in Prostate Cancer in the Era of Magnetic Resonance Imaging-targeted Biopsy: A Large Multicenter Cohort Study. Eur Urol Focus 2021;7:1002-10.

59. Gupta RT, Spilseth B, Patel N, Brown AF, Yu J. Multiparametric prostate MRI: focus on T2-weighted imaging and role in staging of prostate cancer. Abdom Radiol (NY) 2016;41:831-43.
60. Mugler JP 3rd. Optimized three-dimensional fast-spin-echo MRI. J Magn Reson Imaging 2014;39:745-67.
61. Woo S, Suh CH, Kim SY, Cho JY, Kim SH. The Diagnostic Performance of MRI for Detection of Lymph Node Metastasis in Bladder and Prostate Cancer: An Updated Systematic Review and Diagnostic Meta-Analysis. AJR Am J Roentgenol 2018;210:W95-W109.
62. Feutren T, Herrera FG. Prostate irradiation with focal dose escalation to the intraprostatic dominant nodule: a systematic review. Prostate Int 2018;6:75-87.
63. Monninkhof EM, van Loon JWL, van Vulpen M, Kerkmeijer LGW, Pos FJ, Haustermans K, van den Bergh L, Isebaert S, McColl GM, Smeenk RJ, Noteboom J, Walraven I, Peeters PHM, van der Heide UA. Standard whole prostate gland radiotherapy with and without lesion boost in prostate cancer: Toxicity in the FLAME randomized controlled trial. Radiother Oncol 2018;127:74-80.
64. Scheffler K, Hennig J. Is TrueFISP a gradient-echo or a spin-echo sequence? Magn Reson Med 2003;49:395-7.
65. Bjerre T, Crijns S, af Rosenschöld PM, Aznar M, Specht L, Larsen R, Keall P. Three-dimensional MRI-linac intra-fraction guidance using multiple orthogonal cine-MRI planes. Phys Med Biol 2013;58:4943-50.
66. Pathmanathan AU, Schmidt MA, Brand DH, Kousi E, van As NJ, Tree AC. Improving fiducial and prostate capsule visualization for radiotherapy planning using MRI. J Appl Clin Med Phys 2019;20:27-36.
67. Pathmanathan AU, McNair HA, Schmidt MA, Brand DH, Delacroix L, Eccles CL, Gordon A, Herbert T, van As NJ, Huddart RA, Tree AC. Comparison of prostate delineation on multimodality imaging for MR-guided radiotherapy. Br J Radiol 2019;92:20180948.
68. Tyagi N, Fontenla S, Zelefsky M, Chong-Ton M, Ostergren K, Shah N, Warner L, Kadbi M, Mechalakos J, Hunt M. Clinical workflow for MR-only simulation and planning in prostate. Radiat Oncol 2017;12:119.
69. Tyagi N, Fontenla S, Zhang J, Cloutier M, Kadbi M, Mechalakos J, Zelefsky M, Deasy J, Hunt M. Dosimetric and workflow evaluation of first commercial synthetic CT software for clinical use in pelvis. Phys Med Biol 2017;62:2961-75.
70. Dou W, Lin CE, Ding H, Shen Y, Dou C, Qian L, Wen B, Wu B. Chemical exchange saturation transfer magnetic resonance imaging and its main and potential applications in pre-clinical and clinical studies. Quant Imaging Med Surg 2019;9:1747-66.
71. Matsuo M, Matsumoto S, Mitchell JB, Krishna MC, Camphausen K. Magnetic resonance imaging of the tumor microenvironment in radiotherapy: perfusion, hypoxia, and metabolism. Semin Radiat Oncol 2014;24:210-7.
72. Birkhäuser FD, Studer UE, Froehlich JM, Triantafyllou M, Bains LJ, Petralia G, Vermathen P, Fleischmann A, Thoeny HC. Combined ultrasmall superparamagnetic particles of iron oxide-enhanced and diffusion-weighted magnetic resonance imaging facilitates detection of metastases in normal-sized pelvic lymph nodes of patients with bladder and prostate cancer. Eur Urol 2013;64:953-60.
73. Shinmoto H, Tamura C, Soga S, Shiomi E, Yoshihara N, Kaji T, Mulkern RV. An intravoxel incoherent motion diffusion-weighted imaging study of prostate cancer. AJR Am J Roentgenol 2012;199:W496-500.
74. Nelson SJ, Kurhanewicz J, Vigneron DB, Larson PE, Harzstark AL, Ferrone M, et al. Metabolic imaging of patients with prostate cancer using hyperpolarized 1-^{13}Cpyruvate. Sci Transl Med 2013;5:198ra108.
75. Ugurluer G, Atalar B, Zoto Mustafayev T, Gungor G, Aydin G, Sengoz M, Abacioglu U, Tuna MB, Kural AR, Ozyar E. Magnetic resonance image-guided adaptive stereotactic body radiotherapy for prostate cancer: preliminary results of outcome and toxicity. Br J Radiol 2021;94:20200696.
76. Ma TM, Lamb JM, Casado M, Wang X, Basehart TV, Yang Y, Low D, Sheng K, Agazaryan N, Nickols NG, Cao M, Steinberg ML, Kishan AU. Magnetic resonance imaging-guided stereotactic body radiotherapy for prostate cancer (mirage): a phase iii randomized trial. BMC Cancer 2021;21:538.
77. Tetar SU, Bruynzeel AME, Oei SS, Senan S, Fraikin T, Slotman BJ, Moorselaar RJAV, Lagerwaard FJ. Magnetic Resonance-guided Stereotactic Radiotherapy for Localized Prostate Cancer: Final Results on Patient-reported Outcomes of a Prospective Phase 2 Study. Eur Urol Oncol 2021;4:628-34.
78. Alongi F, Rigo M, Figlia V, Cuccia F, Giaj-Levra N, Nicosia L, Ricchetti F, Sicignano G, De Simone A, Naccarato S, Ruggieri R, Mazzola R. 1.5 T MR-guided and daily adapted SBRT for prostate cancer: feasibility, preliminary clinical tolerability, quality of life and patient-reported outcomes during treatment. Radiat Oncol 2020;15:69.

79. Bruynzeel AME, Tetar SU, Oei SS, Senan S, Haasbeek CJA, Spoelstra FOB, Piet AHM, Meijnen P, Bakker van der Jagt MAB, Fraikin T, Slotman BJ, van Moorselaar RJA, Lagerwaard FJ. A Prospective Single-Arm Phase 2 Study of Stereotactic Magnetic Resonance Guided Adaptive Radiation Therapy for Prostate Cancer: Early Toxicity Results. Int J Radiat Oncol Biol Phys 2019;105:1086-94.
80. van Herk M, McWilliam A, Dubec M, Faivre-Finn C, Choudhury A. Magnetic Resonance Imaging-Guided Radiation Therapy: A Short Strengths, Weaknesses, Opportunities, and Threats Analysis. Int J Radiat Oncol Biol Phys 2018;101:1057-60.
81. Murray J, Tree AC. Prostate cancer - Advantages and disadvantages of MR-guided RT. Clin Transl Radiat Oncol 2019;18:68-73.
82. Morita K, Nakaura T, Maruyama N, Iyama Y, Oda S, Utsunomiya D, Namimoto T, Kitajima M, Yoneyama M, Yamashita Y. Hybrid of Compressed Sensing and Parallel Imaging Applied to Three-dimensional Isotropic T2-weighted Turbo Spin-echo MR Imaging of the Lumbar Spine. Magn Reson Med Sci 2020;19:48-55.
83. Delattre BMA, Boudabbous S, Hansen C, Neroladaki A, Hachulla AL, Vargas MI. Compressed sensing MRI of different organs: ready for clinical daily practice? Eur Radiol 2020;30:308-19.
84. Baltzer PA, Renz DM, Herrmann KH, Dietzel M, Krumbein I, Gajda M, Camara O, Reichenbach JR, Kaiser WA. Diffusion-weighted imaging (DWI) in MR mammography (MRM): clinical comparison of echo planar imaging (EPI) and half-Fourier single-shot turbo spin echo (HASTE) diffusion techniques. Eur Radiol 2009;19:1612-20.
85. Gao Y, Han F, Zhou Z, Cao M, Kaprealian T, Kamrava M, Wang C, Neylon J, Low DA, Yang Y, Hu P. Distortion-free diffusion MRI using an MRI-guided Tri-Cobalt 60 radiotherapy system: Sequence verification and preliminary clinical experience. Med Phys 2017;44:5357-66.
86. In MH, Posnansky O, Speck O. High-resolution distortion-free diffusion imaging using hybrid spin-warp and echo-planar PSF-encoding approach. Neuroimage 2017;148:20-30.
87. Franiel T, Hamm B, Hricak H. Dynamic contrast-enhanced magnetic resonance imaging and pharmacokinetic models in prostate cancer. Eur Radiol 2011;21:616-26.
88. Liu Y, Lei Y, Wang Y, Shafai-Erfani G, Wang T, Tian S, Patel P, Jani AB, McDonald M, Curran WJ, Liu T, Zhou J, Yang X. Evaluation of a deep learning-based pelvic synthetic CT generation technique for MRI-based prostate proton treatment planning. Phys Med Biol 2019;64:205022.
89. Persson E, Gustafsson C, Nordström F, Sohlin M, Gunnlaugsson A, Petruson K, Rintelä N, Hed K, Blomqvist L, Zackrisson B, Nyholm T, Olsson LE, Siversson C, Jonsson J. MR-OPERA: A Multicenter/Multivendor Validation of Magnetic Resonance Imaging-Only Prostate Treatment Planning Using Synthetic Computed Tomography Images. Int J Radiat Oncol Biol Phys 2017;99:692-700.
90. Hall WA, Paulson ES, van der Heide UA, Fuller CD, Raaymakers BW, Lagendijk JJW, et al. The transformation of radiation oncology using real-time magnetic resonance guidance: A review. Eur J Cancer 2019;122:42-52.
91. Stemkens B, Paulson ES, Tijssen RHN. Nuts and bolts of 4D-MRI for radiotherapy. Phys Med Biol 2018;63:21TR01.
92. Yuan J, Wong OL, Zhou Y, Chueng KY, Yu SK. A fast volumetric 4D-MRI with sub-second frame rate for abdominal motion monitoring and characterization in MRI-guided radiotherapy. Quant Imaging Med Surg 2019;9:1303-14.
93. Bertholet J, Knopf A, Eiben B, McClelland J, Grimwood A, Harris E, Menten M, Poulsen P, Nguyen DT, Keall P, Oelfke U. Real-time intrafraction motion monitoring in external beam radiotherapy. Phys Med Biol 2019;64:15TR01.
94. Feng L, Tyagi N, Otazo R. MRSIGMA: Magnetic Resonance SIGnature MAtching for real-time volumetric imaging. Magn Reson Med 2020;84:1280-92.
95. van de Lindt T, Sonke JJ, Nowee M, Jansen E, van Pelt V, van der Heide U, Fast M. A Self-Sorting Coronal 4D-MRI Method for Daily Image Guidance of Liver Lesions on an MR-LINAC. Int J Radiat Oncol Biol Phys 2018;102:875-84.
96. Freedman JN, Collins DJ, Gurney-Champion OJ, McClelland JR, Nill S, Oelfke U, Leach MO, Wetscherek A. Super-resolution T2-weighted 4D MRI for image guided radiotherapy. Radiother Oncol 2018;129:486-93.
97. Meyer P, Noblet V, Mazzara C, Lallement A. Survey on deep learning for radiotherapy. Comput Biol Med 2018;98:126-46.
98. Lundervold AS, Lundervold A. An overview of deep learning in medical imaging focusing on MRI. Z Med Phys 2019;29:102-27.
99. Hyun CM, Kim HP, Lee SM, Lee S, Seo JK. Deep learning for undersampled MRI reconstruction. Phys Med

Biol 2018;63:135007.
100. Terpstra ML, Maspero M, d'Agata F, Stemkens B, Intven MPW, Lagendijk JJW, van den Berg CAT, Tijssen RHN. Deep learning-based image reconstruction and motion estimation from undersampled radial k-space for real-time MRI-guided radiotherapy. Phys Med Biol 2020;65:155015.
101. Nie D, Trullo R, Lian J, Petitjean C, Ruan S, Wang Q, Shen D. Medical Image Synthesis with Context-Aware Generative Adversarial Networks. Med Image Comput Comput Assist Interv 2017;10435:417-25.
102. Turkbey B, Choyke PL. PI-QUAL, a New System for Evaluating Prostate Magnetic Resonance Imaging Quality: Is Beauty in the Eye of the Beholder? Eur Urol Oncol 2020;3:620-1.
103. de Rooij M, Israël B, Tummers M, Ahmed HU, Barrett T, Giganti F, Hamm B, Løgager V, Padhani A, Panebianco V, Puech P, Richenberg J, Rouvière O, Salomon G, Schoots I, Veltman J, Villeirs G, Walz J, Barentsz JO. ESUR/ESUI consensus statements on multi-parametric MRI for the detection of clinically significant prostate cancer: quality requirements for image acquisition, interpretation and radiologists' training. Eur Radiol 2020;30:5404-16.

Cite this article as: Yuan J, Poon DMC, Lo G, Wong OL, Cheung KY, Yu SK. A narrative review of MRI acquisition for MR-guided-radiotherapy in prostate cancer. Quant Imaging Med Surg 2022;12(2):1585-1607. doi: 10.21037/qims-21-697

